



PSU/PET copolymer-based asymmetric polymeric membranes: influence of antioxidant

Smitha Rajesh, Z.V.P. Murthy*

Department of Chemical Engineering, Sardar Vallabhbhai National Institute of Technology, Surat 395007, Gujarat, India, email: smitharps@gmail.com (S. Rajesh), Tel. +91 261 2201648, 2201642; Fax: +91 261 2227334; emails: zvp2000@yahoo.com, zvp2000@ched.svnit.ac.in (Z.V.P. Murthy)

Received 27 July 2015; Accepted 9 November 2015

ABSTRACT

Aim of this work was to synthesize thermally and mechanically stable ultrafiltration polymeric membranes. The preparation (phase inversion method) and characteristics of asymmetric polysulfone/polyethylene terephthalate (PSU/PET) copolymer membranes are studied in detail. Polymeric membranes were synthesized from the casting solutions of PSU/PET, dichloromethane solvent and 2,2'-ethylidene-bis(4,6-di-*tert*-butylphenol) (EBBP) as antioxidant along with water-soluble poly(ethylene glycol) (PEG) as an additive through *in situ* process. From experiments, it is observed that when the antioxidant EBBP quantity reached 15 g (15 wt%), the morphologies and properties of resultant membranes are excellent. It was observed that antioxidant EBBP, along with PEG, behaves as pore-forming agent to enhance pure water flux and reduce solute rejection of membranes, but further increase in antioxidant EBBP resulted in pore-reduction. The membrane were analyzed using scanning electron microscopy, Fourier transform infrared spectroscopy, mechanical strength evaluation and cross-flow filtration for milk concentration and contact angle. The results indicated that the addition of antioxidant EBBP results to a thermally stable membrane. Presence of antioxidant affected the mechanical strength, surface roughness, and membrane morphology.

Keywords: Polysulfone/polyethylene terephthalate; Poly(ethylene glycol); Phase inversion, 2,2'-ethylidene-bis(4,6-di-*tert*-butylphenol); Asymmetric membrane

1. Introduction

Polymers are extensively used for the manufacturing of good quality membranes. The end use of these membranes is carried out by ultrafiltration (UF), microfiltration (MF), nanofiltration (NF), and reverse osmosis (RO) operations, ranging from 10 Å to 0.2 µm,

having good resistance to chemicals like acids, aliphatic hydrocarbons and alcohols. For processing the polymer, stable properties are to be identified and it is to be analyzed that the properties will be retained after processing. The simplest method for the preparation of asymmetric polymer membranes is phase inversion method. This method is refined a lot of times and as on date it is very simple to understand the formation mechanism. By this technique, thin layer

*Corresponding author.

of polymer casting solution is cast on a preferred substrate and later dipped into a coagulation bath. The formation of membrane happens by the diffusion exchange of solvent and non-solvent resulting in to phase separation [1,2]. The characteristic morphology of asymmetric membranes is seen as a dense top layer and a porous sublayer. The asymmetric membranes are regularly applied for gas as well as solution separation. This is because the skin layer works as selective barrier film to the permeation of solute through membrane and the porous sublayer provides good mechanical strength to the membrane.

Because of the excellent chemical resistance to various chemicals, physical and thermal stability even in adverse conditions, polysulfone (PSU) and polyethylene terephthalate (PET) are generally used for membrane manufacturing [3,4]. The morphology and other properties of PSU/PET asymmetric membranes can be controlled by dissolving a third component as additive along with polymer and solvent in the casting solution itself. The use of poly(ethylene glycol) (PEG) as an additive is known and use of 2,2'-ethylidene-bis(4,6-di-*tert*-butylphenol) (EBBP) an antioxidant, as additive is well established by various researchers [5–7]. Many scientists had studied and explained the effect of additives in terms of their physical and chemical characteristics such as water solubility, activity, and surface tension [8]. Additives are basically pore-forming agents, which enhance membrane fluxes. This significantly reduces the rejection capability of prepared membranes.

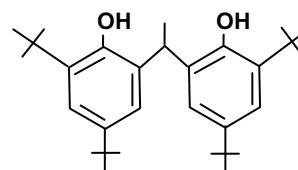
In the current work, membrane casting solutions are prepared by taking PEG of a particular molecular weight (MW 6,000), by analyzing the effect of molecular weight of PEG on the viscosity of the casting solution, along with different compositions of antioxidant EBBP, and constant ratio (1:1) of PSU/PET in dichloromethane (DCM) solvent. Effects of antioxidant EBBP and additive PEG on thermal and mechanical properties of membranes are studied in detail. The membrane formation mechanism was discussed in detail to understand the role of combination of additive PEG and antioxidant EBBP, mobility due to the presence of PEG and the affinity between PEG and EBBP compounds with membrane casting solutions.

2. Experimental

All the chemicals, if not mentioned otherwise, are obtained from Sigma–Aldrich. PEG6000 is used as an additive. The EBBP is incorporated as an antioxidant. Distilled water was used for all the experimental purpose.

2.1. *In situ* membrane synthesis

Membranes were synthesized by phase inversion process at room temperature (25°C). By dissolving measured quantities of polysulfone/polyethylene terephthalate (PSU/PET) in DCM, the casting solutions were prepared and stirred for one hour at ambient conditions. This polymer casting solution was poured into a glass bottle (~6 h) and kept at ambient temperature to remove the air bubbles. Then EBBP, whose structure is given below, as an antioxidant and water-soluble poly(ethylene glycol) (PEG) as an additive in different weight ratios, were added and stirring was continuously done until the polymer casting solution was totally dissolved and become homogeneous.



Structure of EBBP

The resultant polymer casting solution was again kept in a glass bottle (~6 h) and stored at room temperature to remove the air bubbles. The composition and viscosity details of the resultant casting solutions are given in Table 1. Casting solutions were cast into thin films (~150 μm thick) on Teflon sheets, and then the wet films were immersed into a water bath immediately for gelation. The gelation was completed in approximately 15 min and the membranes formed are further kept immersed in distilled water for one day. Then the membranes were soaked in ethanol for 4 h and dried at room temperature. The membranes were inspected visually for defects and non-defected areas were used for characterization.

2.2. Membrane characterization

2.2.1. SEM studies

Scanning electron microscopy (SEM) was used for studying membrane cross-sectional and surface morphologies. Liquid nitrogen-treated membranes were coated with gold under vacuum before analysis. The membranes were well dried and residues of PEG and EBBP were characterized by evaluating total reflection-Fourier transform infrared (ATR-FTIR) spectroscopy (Bruker Vector 22 FT-IR spectrometer, Germany).

Table 1
The compositions and viscosities of PSU/PET, EBBP, PEG, DCM solutions

Membrane	Casting solution		
	DCM, PEG, EBBP, PSU/PET (in weight ratio)	Molecular weight of PEG	Viscosity (Pa s)
I	75/5/5/10	6,000	8.20
II	75/5/10/10	6,000	8.65
III	75/5/15/10	6,000	9.00
IV	75/5/20/10	6,000	9.34
V	75/5/25/10	6,000	9.62

2.2.2. Surface pore size and porosity measurements

The porosity of the membranes was measured by measuring the thickness (D), area (A), and mass (W_m) of membranes and polymer density (ρ_p). Dried membranes (48 h in atmosphere) is kept in vacuum oven at 25°C again for 48 h. Membrane thickness and mass were evaluated using thickness gauge, SEM, and electronic balance. The porosity percentage was measured using below equation:

$$\text{Porosity (\%)} = \left[\frac{DA - \left(\frac{W_m}{\rho_p} \right)}{DA} \right] \times 100\% \quad (1)$$

Pure water flux and solute rejection measurements were measured using an UF cell with 24 cm² effective

membrane area at ambient temperature. Pure water flux measurements were carried out using distilled water as permeate.

2.2.3. Flux and retention

The synthesized membrane performance was studied using cross-flow system [6,7]. The cross-flow system consists of essential parts, such as pressure regulators, pump, reservoir, valves, and UF cells. The details of the experimental setup are shown in Fig. 1 [9]. The retentate was re-circulated to the reservoir and permeate was collected and weighed. The cross-flow cell holds flat sheet membrane having an effective area of 24 cm². The pasteurized milk after homogenization (2.5% of protein and 1.2% of fat) was used as the feed for evaluating performance of

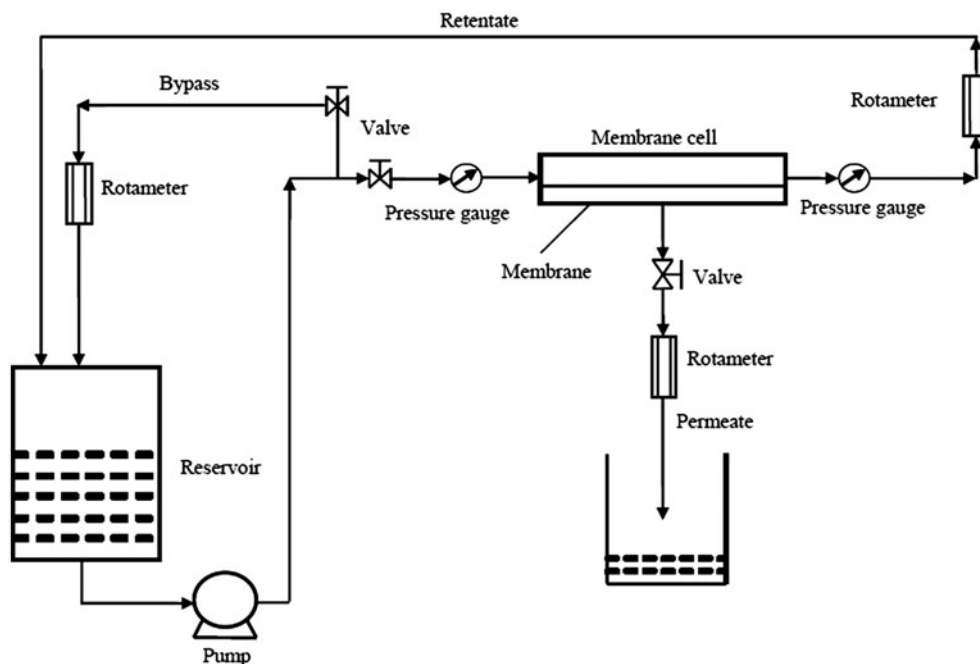


Fig. 1. Cross-flow filtration for determining pure water and milk water permeation.

membrane and fouling. All the experiments were conducted at ambient temperature (25°C). Before the experiments, membranes were pre-compressed with pure water at 50 psig for 1 h to avoid compaction of membrane during separation operation and then the membrane flux was measured at a feed flow rate of 5 L/min (or flow velocity of 2 m/s) and 50 psig after 1 h. Since the fat molecules cannot pass through the membrane, the focus was on protein retention. By measuring the amount of protein in the permeate using the standard Bradford method [10], protein rejection by membrane was calculated. The experimentally obtained rejection, R , is defined as:

$$R = \left[1 - \frac{C_p}{C_f} \right] \times 100\% \quad (2)$$

where C_p and C_f are the protein concentration in the permeate and feed, respectively.

2.2.4. Mechanical properties

The mechanical properties of the synthesized membranes were measured using Shimadzu AG-10-TB tensile test machine, according to ASTM D882. All the samples were cut in to the required shape before testing at 25°C [9]. Average values of tests of three samples were used and reported for elongation and tensile strength.

2.2.5. Contact angle analysis

Sessile drop method using Goniometer (Rame-Hart Inc. Imaging System, USA) was used to measure equilibrium contact angles of water with membranes in saturated environment. Stainless-steel holder is used to mount flat sheets to place in a chamber. With the help of a glass syringe with a stainless-steel needle, liquid drop is placed on the membrane. The angles were measured with RHI

software and by taking images with attached video camera [11]. Around 5 min stabilization time was allowed to capture the image. Within 1 s approximately 50 readings were recorded and average of these readings was used to estimate contact angle. Five readings were noted for each drop of liquid on the same membrane surface and average of these values was recorded.

3. Results and discussion

3.1. Membrane permeation properties and morphologies

Permeability and structure of PSU/PET membranes with PEG and different EBBP composition are shown in Table 2. The membrane is prepared with 1:1 ratio of PSU and PET in the same conditions and characterized with same methods. With increase in EBBP antioxidant quantity, water flux, membrane thickness and porosity initially increased and then decreased, but still higher than that of membrane synthesized without any antioxidant. The water flux, protein rejection, thickness, and porosity of the membrane synthesized without any additive and antioxidant are 15 L/(m² h), 43.4%, 32 μm and 44%, respectively. Protein rejection initially decreased, and reached to the lowest and then to a minimum and then increased a little. The best point needed to be noted here is that all these membranes show good UF properties.

3.2. SEM

From SEM images, efforts have been made to understand the cross-sectional and the upper surface of membranes. Fig. 2 shows the cross-sectional images of membranes and Fig. 3 shows the upper surface images of membranes. Fig. 2 showed the characteristics of an asymmetric membrane having top surface with a skin layer and a porous supporting solid matrix, antioxidant along with PEG as additives exerted noticeable effect on membrane surface and cross section. The size and number of pores on the membrane upper surface increased when the weight

Table 2
Properties and performance of membranes

Membrane	Thickness (μm)	Porosity (%)	Water flux (L/(m ² h))	Protein rejection (%)
I	41	69.7	52	86.8
II	43	72.3	69	81.2
III	58	80.6	138	74.2
IV	44	77.5	129	80.2
V	42	67.2	82	82.8

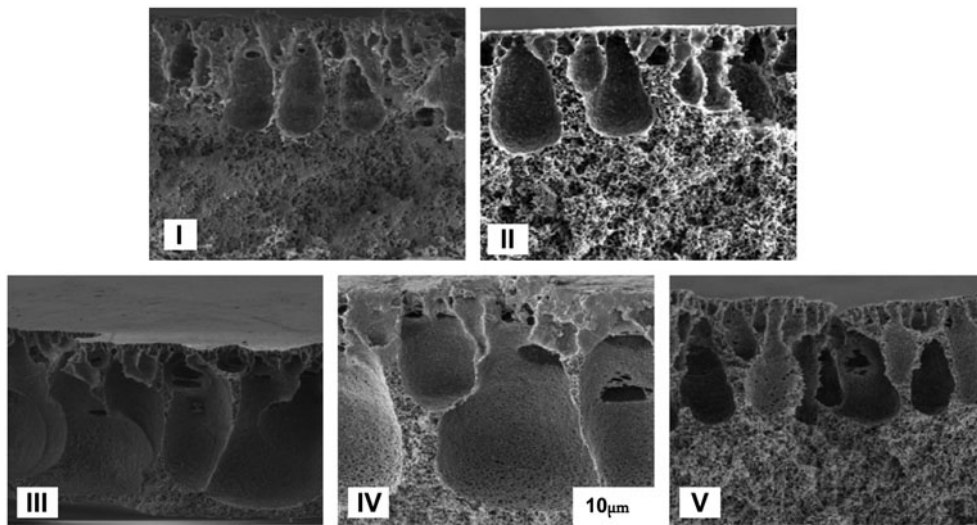


Fig. 2. Cross-sectional SEM images (10 μm) of membranes I, II, III, IV, and V.

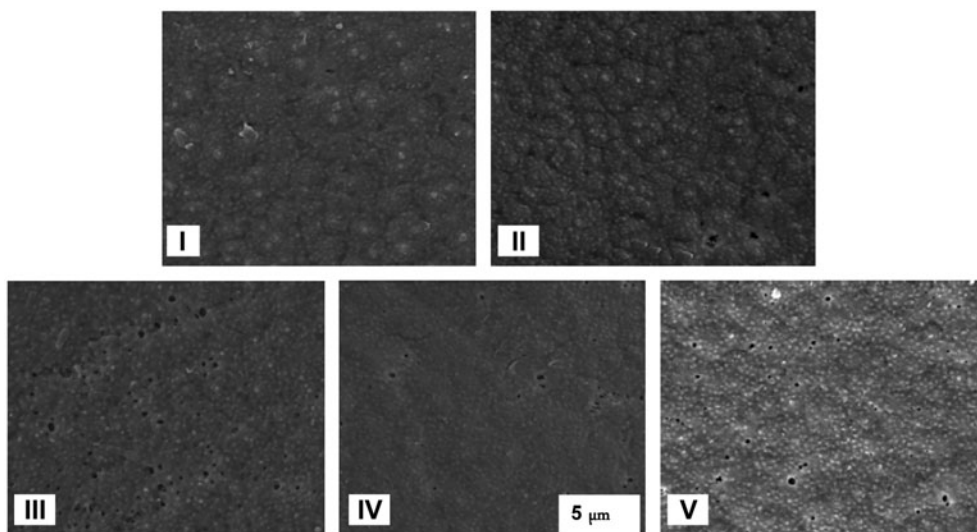


Fig. 3. Upper surface SEM images (5 μm) of membrane I, II, III, IV, and V.

of antioxidant EBBP increased from 5 to 15 wt%. On further increase in antioxidant EBBP content, the pore size and pore number of the upper surface declined. The variation trend of macrovoid growth in the membrane cross section was similar to that of the pores on the membrane upper surface. The finger-like cavities grew gradually with increase in antioxidant content. The finger-like pores expanded in breadth and length toward the membrane bottom when antioxidant EBBP weight reached to 15 g. From Fig. 2(I), (II), and (III), it is obvious that along with this the wall of finger-like macrovoids changed from a dense to porous morphology and the sponge-like structure underneath

the finger-like pores became more porous and interconnected. When the antioxidant content gets increased further, the finger-like pores were suppressed and the sponge-like structures were developed although the macrovoids wall presented a more porous structure as shown in Fig. 2(IV) and (V). It could be concluded from SEM images observations of membranes that the membranes morphologies and structure agreed well with permeation results that depend on not only the overall membranes morphologies but also especially the upper surface of membranes. Generally, more pores on membrane surface and the better interconnectivity inside membrane

would contribute to enhancing pure water flux and reducing solute rejection [12,13]. When antioxidant EBBP weight increased from 5 to 25 wt%, the pore size and pore number on membrane upper surface initially increased (Fig. 3), and then declined slightly. Correspondingly, pure water fluxes increased initially, and then decreased, and protein rejections reduced initially, then slightly increased. The membrane thickness and porosity also depend on the membrane morphology and structure. The sufficient development of macrovoids and interconnectivity leads to the increase in the membrane thickness and porosity. As antioxidant EBBP weight increased from 5 to 25 wt%, the macrovoids were developed initially and then were suppressed, so the thickness of membranes increased initially, and then decreased. It could be deduced from the above analysis that antioxidant acted as a pore-forming agent when it is present in lower quantity, whereas increase in antioxidant quantity could suppress the growth of finger-like macrovoids. The membranes are soaked for 5 d, and during this period the pore formation mechanism on membrane surface proposed by previous studies could explain the top surface morphology of these resultant membranes [14–16].

3.3. Membrane surface porosity and pore size distribution

Porosity is measured and results are combined in Table 2. The antioxidant EBBP incorporated membranes show slight increase in porosity and as the antioxidant content increased the porosity of the membrane also got increased. This may be because of the stronger adsorption of antioxidant EBBP which might cause the pore to open and porosity increase. This explains the reason behind pore size increase in membranes with antioxidant.

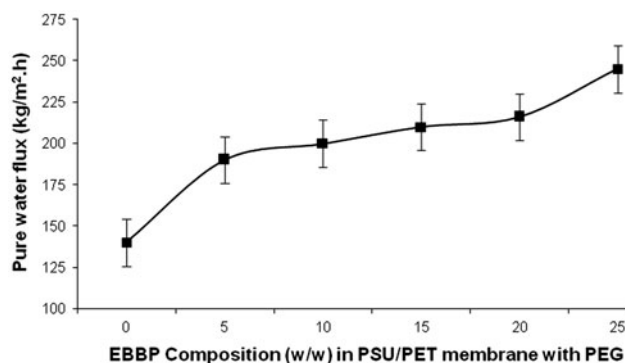


Fig. 4. Effect of EBBP composition on membrane pure water flux.

3.4. Performance of membrane

Fig. 4 indicates the influence of the PSU/PET copolymer with additive PEG and varying concentration of antioxidant EBBP on the pure water permeability. Increase in pure water flux of membranes observed from 190 to 245 kg/m² h with increase in antioxidant EBBP content in the casting solution from 5 to 25%.

Fig. 5 indicates the increase in milk water permeation of PSU/PET membrane with additive PEG and different compositions of antioxidant EBBP. Fig. 5 indicates that the milk water permeation of PSU/PET membranes with additive PEG and antioxidant EBBP is also increasing on increasing antioxidant content in it. Antioxidant EBBP addition increased the hydrophilicity of copolymer-based membranes and brought a difference in the surface and sublayer morphology. In other words, the pore size of the membrane influences the water flux, the hydrophilicity, and the pore density, and the membrane permeability is influenced by the surface porosity of membranes [17]. The pore size of PSU/PET membrane with higher antioxidant EBBP content was larger, and the surface porosity, hydrophilicity, and pore density of membrane were found excellent. This was the reason for higher milk water permeability and water flux in synthesized PSU/PET membranes.

In order to study the flux behavior of the membranes with antioxidant EBBP 5, 10, 15, 20, 25, and 0% composition of PSU/PET were analyzed. Homogenized milk with 2.5% protein and 1.2% fat was the feed solution. Fig. 6 shows the flux behavior of PSU/PET membranes with time, where line VI represents 0% EBBP. The PSU/PET blend membranes flux increases with increase in EBBP content in it.

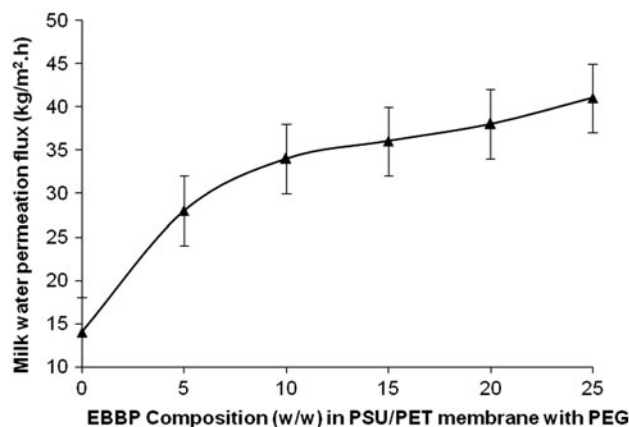


Fig. 5. Effect of EBBP composition on milk water permeation.

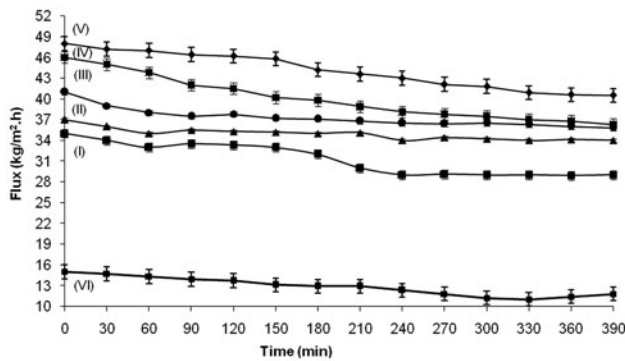


Fig. 6. Flux behavior of membranes I, II, III, IV, V, and VI (Membrane VI has no EBBP).

Membrane non-fouling properties can be measured by analyzing the capability to restore its water flux even after subjected to foulants. The larger the flux value, easier the desorption of the foulants from the membrane [18–20]. The recovery figure shows that the PSU/PET copolymer-based membrane surface was low-fouling in nature.

Hydrophilicity, higher pore density, and surface porosity of PSU/PET membranes lead to higher flux. It is evident from above details that there is huge difference between fouling tendencies on addition of antioxidant to the membranes. Hydrophilicity of membrane can be considered as the main characteristics responsible for membrane fouling resistance [21,22]. Membrane hydrophilicity improved the membranes fouling resistance.

3.5. Fouling resistance of PSU/PET membranes with EBBP

Flux recovery of membrane with antioxidants is calculated along membrane resistance (R_m) and cake resistance of the layer formed on surface of the membrane (R_c). Further total filtration resistance (R_t) is calculated by adding fouling resistance due to pore plugging and irreversible adsorption of foulants on the membrane pore wall or surface (R_f) to membrane

resistance and cake resistance [12]. Flux recovery was calculated from the following relation [12]:

$$\text{Flux recovery (\%)} = \frac{J_{ww}}{J_{wi}} \times 100 \quad (3)$$

where J_{ww} is the pure water flux of fouled membrane and J_{wi} is the pure water flux of virgin membranes. Fouling is expressed by the resistance which appears during filtration process. Because of the formation of cake or gel layer on the surface of membrane, resistance to filtration takes place. The flux (J), through the cake and the membrane, is explained by Darcy's law:

$$J = \frac{\Delta P}{\mu \sum R} \quad (4)$$

where ΔP , μ , and $\sum R$ or R_t are transmembrane pressure, viscosity of permeate, and sum of the resistances, respectively. The intrinsic membrane resistance (R_m) is calculated using initial pure water flux [12]:

$$R_m = \frac{\Delta P}{\mu J_{wi}} \quad (5)$$

Fouling resistance (R_f), due to pore plugging and irreversible adsorption of foulants on membrane pore wall or surface, is calculated by [12]:

$$R_f = \frac{\Delta P}{\mu J_{ww}} - R_m \quad (6)$$

Cake resistance, R_c , due to the formation of cake or gel layer on the surface of membrane, can be derived from the water flux values obtained after chemical cleaning:

$$R_c = \frac{\Delta P}{\mu J_m} - R_m - R_f \quad (7)$$

Table 3
Filtration resistances (m^{-1}) of membranes

Membrane	Flux recovery (%)	R_m ($\times 10^{11}$)	R_f ($\times 10^{11}$)	R_c ($\times 10^{11}$)	R_t ($\times 10^{11}$)
I	78	0.74	0.17	3.37	4.28
II	81	0.58	0.14	3.28	4.00
III	83	0.56	0.14	3.26	3.96
IV	86	0.54	0.13	3.22	3.89
V	88	0.52	0.12	3.20	3.84

Table 4
The mechanical properties the synthesized membranes

Membrane	Elongation at break (%)	Tensile strength (MPa)
I	18.6	3.7
II	19.8	3.9
III	21.5	4.1
IV	22.2	4.6
V	25.3	5.2

where J_m is the milk water flux.

The total filtration resistance (R_t) can be calculated as:

$$R_t = R_m + R_f + R_c \quad (8)$$

The calculated R_m , R_f , R_c , and R_t were shown in Table 3.

The flux recovery was used to understand the recycling property of PSU/PET and antioxidant EBBP membranes. The flux recovery of PSU/PET membrane without any additive or antioxidant is having a total filtration resistance of more than 5×10^{-11} . The flux recovery value of PSU/PET membrane with antioxidant EBBP was getting higher as EBBP content gets increased. Results of experiments clearly indicated that cake or gel layer formation on the surface of membrane was the main reason for fouling mechanism [12,17]. It can be observed from Table 3 that the various filtration resistances of PSU/PET membranes with higher antioxidant EBBP content are lower than membranes with lower antioxidant content. The membrane surface properties like roughness and hydrophilicity are the major factors for identifying the cake layer resistance [23,24]. In short, the surface properties of the copolymer membranes were significantly improved by adding additive PEG and antioxidant EBBP.

3.6. Mechanical properties of membranes

Table 4 shows the mechanical properties like tensile strength and elongation at break of PSU/PET membranes with PEG and EBBP. The results indicated that the mechanical properties of the membranes are improved by the incorporation of antioxidant in to the casting solution at different compositions. Thus, the incorporation of antioxidant EBBP into the casting solution increases the mechanical properties of copolymer-based membranes by decreasing the membrane brittleness, and thus increases membranes stability and maintains esthetics look.

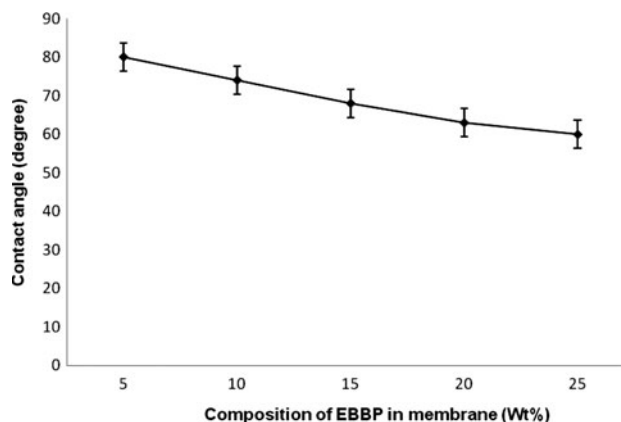


Fig. 7. Effect of EBBP composition on membrane contact angle.

3.7. Contact angle analysis

The contact angles of water on antioxidant EBBP incorporated copolymer-based membranes were evaluated and results were described in Fig. 7. Contact angle measurement is carried to measure the hydrophilicity of the polymer membrane surface [25]. It can be concluded that with increase in antioxidant EBBP composition the contact angle is reducing marginally. This indicates that when antioxidant EBBP content in a polymeric membrane increases, the hydrophilicity of the polymeric membrane also increases. Hence, membranes on the addition of antioxidant EBBP converts it from hydrophobic to more hydrophilic, as observed from increase in contact angle values.

4. Conclusions

The current research work shows that the addition of antioxidant EBBP with additive PEG could change the PSU/PET membrane structure and properties. The membrane preparation system was studied in detail to understand the influence of EBBP concentration on the copolymer and the affinity between EBBP and PEG with the copolymer. A viscosity enhancement of

casting solution is observed during the phase inversion process due to the presence of antioxidant EBBP and PEG. This had resulted in delayed phase separation, and the top membrane surface formed was relatively dense with residual additive and antioxidant. The macrovoid growth or suppression was controlled by the trade-off between PEG molecular chain length and the affinity between PEG and casting solution. The copolymer mobility is improved by the presence of PEG with EBBP and this has resulted in decrease in affinity between EBBP and casting solutions. This had helped EBBP and PEG for entering into the nuclei of lean polymer phase. This has resulted in casting solution in front of nuclei became stable and favored the nuclei to expand to the larger finger-like pores. But when EBBP quantity got increased and reached up to 15 g (15 wt%), it prevented diffusion to the nuclei. This resulted into a sponge-like structure and further number of pores increased. *In situ* addition of antioxidant was studied in order to further enhance the thermal properties of the membranes. Due to modification of structure, the hydrophilicity of PSU membrane is also improved by incorporating PSU/PET with PEG and EBBP. This resulted in a mechanically and thermally stable membrane base. Pure water flux, milk water permeation, and anti-fouling properties of membranes are increased with increase in EBBP composition in the casting solution. The prepared membranes are comparatively non-fouling and having improved fluxes with higher mechanical strength. The sufficient development of macrovoids and interconnectivity results in the increase in the membrane thickness and porosity.

References

- [1] C.M. Zimmerman, A. Singh, W.J. Koros, Tailoring mixed matrix composite membranes for gas separations, *J. Membr. Sci.* 137 (1997) 145–154.
- [2] M.M. Teoh, T.S. Chung, K.Y. Wang, D. Michael, M.D. Guiver, Exploring Torlon/P84 co-polyamide-imide blended hollow fibers and their chemical cross-linking modifications for pervaporation dehydration of isopropanol, *Sep. Purif. Technol.* 61 (2008) 404–413.
- [3] H. Matsuyama, T. Maki, M. Teramoto, K. Kobayashi, Effect of PVP additive on porous polysulfone membrane formation by immersion precipitation method, *Sep. Sci. Technol.* 38 (2003) 3449–3458.
- [4] T. Tweddle, O. Kutowy, W. Thayer, S. Sourirajan, Polysulfone ultrafiltration membranes, *Ind. Eng. Chem. Prod. Res. Dev.* 22 (1983) 320–326.
- [5] Y. Liu, G.H. Koops, H. Strathmann, Characterization of morphology controlled polyethersulfone hollow fiber membranes by the addition of polyethylene glycol to the dope and bore liquid solution, *J. Membr. Sci.* 223 (2003) 187–199.
- [6] A. Idris, K.Y. Lee, The effect of different molecular weight PEG additives on cellulose acetate asymmetric dialysis membrane performance, *J. Membr. Sci.* 280 (2006) 920–927.
- [7] J.H. Kim, K.H. Lee, Effect of PEG additive on membrane formation by phase inversion, *J. Membr. Sci.* 138 (1998) 153–163.
- [8] S.S. Madaeni, A. Rahimpour, J. Barzin, Preparation of polysulfone ultrafiltration membranes for milk concentration: Effect of additives on morphology and performance, *Iran. Polym. J.* 14 (2005) 421–428.
- [9] S. Rajesh, Z.V.P. Murthy, In situ synthesis and characterization of 2,2'-methylenebis(6-tert-butyl-4-ethylphenol) incorporated polymeric membranes, *Adv. Polym. Technol.* 33 (2014) Article 21392, and 34 (2015) 21513.
- [10] M.M. Bradford, A rapid and sensitive method for the quantitation of microgram quantities of protein utilizing the principle of protein-dye binding, *Anal. Biochem.* 72 (1976) 248–254.
- [11] M.K. Mandal, S. Dutta, P.K. Bhattacharya, Characterization of blended polymeric membranes for pervaporation of hydrazine hydrate, *Chem. Eng. J.* 138 (2008) 10–19.
- [12] A. Rahimpour, S.S. Madaeni, S. Mehdipour-Ataei, Synthesis of a novel poly(amide-imide) (PAI) and preparation and characterization of PAI blended polyethersulfone (PES) membranes, *J. Membr. Sci.* 311 (2008) 349–359.
- [13] C. Bangxiao, Y. Li, Y. Hailin, G. Congjie, Effect of separating layer in pervaporation composite membrane for MTBE/MeOH separation, *J. Membr. Sci.* 194 (2001) 151–156.
- [14] A. Tabe-Mohammadi, J.P.G. Villaluenga, H.J. Kim, T. Chan, V. Rauw, Effects of polymer solvents on the performance of cellulose acetate membranes in methanol/methyl tertiary butyl ether separation, *J. Appl. Polym. Sci.* 82 (2001) 2882–2895.
- [15] M. Yoshikawa, T. Yoshioka, J. Fujime, A. Murakami, Pervaporation of methanol/methyl-tert-butyl ether mixtures through agarose/hydroxyethylcellulose blended membranes, *J. Appl. Polym. Sci.* 86 (2002) 3408–3411.
- [16] J. Barzin, S.S. Madaeni, H. Mirzadeh, M. Mehrabzadeh, Effect of polyvinylpyrrolidone on morphology and performance of hemodialysis membranes prepared from polyether sulfone, *J. Appl. Polym. Sci.* 92 (2004) 3804–3813.
- [17] Z.L. Xu, F.A. Qusay, Effect of polyethylene glycol molecular weights and concentrations on polyethersulfone hollow fiber ultrafiltration membranes, *J. Appl. Polym. Sci.* 91 (2004) 3398–3407.
- [18] T.P. Hou, S.H. Dong, L.Y. Zheng, The study of mechanism of organic additives action in the polysulfone membrane casting solution, *Desalination* 83 (1991) 343–360.
- [19] I.C. Kim, K.H. Lee, Effect of various additives on pore size of polysulfone membrane by phase inversion process, *J. Appl. Polym. Sci.* 89 (2003) 2562–2566.
- [20] A. Asatekin, S. Kang, M. Elimelech, A.M. Mayes, Anti-fouling ultrafiltration membranes containing polyacrylonitrile-graft-poly(ethylene oxide) comb copolymer additives, *J. Membr. Sci.* 298 (2007) 136–146.

- [21] S.I. Nakao, S. Yumoto, S. Kimura, Analysis of rejection characteristics of macromolecular gel layer for low molecular weight solutes in ultrafiltration, *J. Chem. Eng. Jpn.* 15 (1982) 463–468.
- [22] Z. Chen, J. Yang, D. Yin, Y. Li, S. Wu, Fabrication of poly(1-vinylimidazole)/mordenite grafting membrane with high pervaporation performance for the dehydration of acetic acid, *J. Membr. Sci.* 349 (2010) 175–182.
- [23] H.A. Mousa, Investigation of UF membranes fouling by humic acid, *Desalination* 217 (2007) 38–51.
- [24] M.A. Aroon, A.F. Ismail, M.M. Montazer-Rahmati, T. Matsuura, Morphology and permeation properties of polysulfone membranes for gas separation: Effects of non-solvent additives and co-solvent, *Sep. Purif. Technol.* 72 (2010) 194–202.
- [25] M. Omidvar, S.M. Mousavi, M. Soltanieh, A.A. Safekordi, Preparation and characterization of poly(ethersulfone) nanofiltration membranes for amoxicillin removal from contaminated water, *J. Environ. Health Sci. Eng.* 12 (2014) Article 18, doi: [10.1186/2052-336X-12-18](https://doi.org/10.1186/2052-336X-12-18).